

An XMM–Newton survey of Extremely Red Objects

M. Brusa¹, A. Comastri², E. Daddi³, A. Cimatti⁴, C. Vignali⁵

¹ Dipartimento di Astronomia, Università di Bologna, via Ranzani 1, I-40127 Bologna, Italy

² INAF – Osservatorio Astronomico di Bologna, via Ranzani 1, I-40127 Bologna, Italy

³ European Southern Observatory, Karl–Schwarzschild–Strasse 2, D–85748 Garching bei Muenchen, Germany

⁴ INAF – Osservatorio Astrofisico di Arcetri, Largo E. Fermi 5, I–55025 Firenze, Italy

⁵ Dept. of Astronomy and Astrophysics, The Pennsylvania State University, 525 Davey Lab, University Park, PA 16802, USA

Abstract. We present preliminary results of a 25 ks XMM–Newton observation of the largest sample of Extremely Red Objects (EROs) available to date (~ 450 sources), selected in a contiguous area of ~ 700 arcmin² (Daddi et al. 2000). Five of the 36 hard X–ray selected sources brighter than 7×10^{-15} erg cm⁻² s⁻¹ in the 2–10 keV band, are associated with EROs. All of the X–ray detected EROs show rather extreme X–ray–to–optical flux ratios, suggesting the presence of highly obscured AGN activity.

1. Introduction

Extremely Red Objects (EROs, $R - K > 5$) were discovered serendipitously a decade ago (Elston et al. 1988) from optical and near–infrared selection criteria. Having the colors expected for high-redshift passive ellipticals, EROs can be used as tracers of distant and old spheroids as a test for different cosmological models.

Recent wide-area surveys have shown that the surface density of EROs is consistent with that expected for elliptical galaxies, assuming pure luminosity evolution (PLE). About 10% of all objects down to a K -band magnitude limit of 19.2 are EROs (Daddi et al. 2000; Daddi, Cimatti & Renzini, 2000). Furthermore, a large angular clustering signal associated with EROs was detected from the K -selected sample over the same area, that is due to the large-scale structure traced by early-type galaxies at $z \sim 1$ (Daddi et al. 2002).

On the other hand, the broad-band properties of EROs are also consistent with those expected for high-redshift dusty starbursts (e.g., HR–10, Cimatti et al. 1998; Smail et al. 1999) and Active Galactic Nuclei (AGN) reddened by dust (Pierre et al. 2001).

The relative fraction of old ellipticals, dusty star-forming systems and obscured AGN among optically selected ERO samples is a key parameter in the study of the galaxy evolution and the link between massive elliptical galaxy in formation and the onset of AGN activity (Almaini et al. 2002; Granato et al. 2001).

A step towards constraining the relative fractions of these different source types within the ERO population has been recently achieved by the $K20$ survey (Cimatti et al. 2002; Daddi et al. 2002) by means of deep VLT spectroscopy. The spectroscopic counterparts of about 45 EROs with $K \leq 19.2$ turned out to be in about equal proportion old, passive ellipticals (31%) and dusty emission-line galaxies (33%) at $z = 0.8 - 1.5$, while a comparable fraction is still unidentified. Interestingly, the average spectrum of the emission-line EROs shows a very red and smooth continuum with [OII] $\lambda 3727$ and a weak [NeV] $\lambda 3426$, suggesting that a fraction of these sources hosts hidden AGN activity.

Given that the Spectral Energy Distribution (SED) of optically obscured type II AGN is dominated by the host galaxy starlight, they show $R - K$ colors similar to those of passive ellipticals; therefore, sensitive hard X–ray observations provide a powerful tool to uncover AGN activity within the ERO population. Indeed, a sizeable fraction of the new population of faint hard X–ray selected sources, recently investigated in *Chandra* and XMM–Newton medium–deep observations, turned out to be faint ($R > 24.5$), obscured objects, with red optical to near–infrared colours (Mushotzky et al. 2000; Cowie et al. 2001; Gandhi et al. 2001; Hornschemeier et al. 2001; Alexander et al. 2002; Mainieri et al. 2002a).

The most extensive study on the X–ray properties of EROs to date was performed by Alexander et al. (2002) using the 1 Ms *Chandra* Deep Field North (CDF-N) observation. Targeting a 70.3 arcmin² region close to the CDF-N aim-point, Alexander et al. (2002) detected X–ray emission from 13 EROs ($21^{+12}_{-8}\%$ of the $K \leq 20.1$ ERO sample). The majority (2/3) of the X–ray detected EROs were found to have X–ray properties consistent with highly obscured AGNs [$N_{\text{H}} \approx (5-35) \times 10^{22}$ cm⁻² for $z = 1-3$]. Moreover, starbursts and normal elliptical galaxies were also possibly detected at the faintest X–ray fluxes. Although having deep X–ray and optical observations, this study is limited in areal coverage, and therefore is unsuitable for detailed statistical and

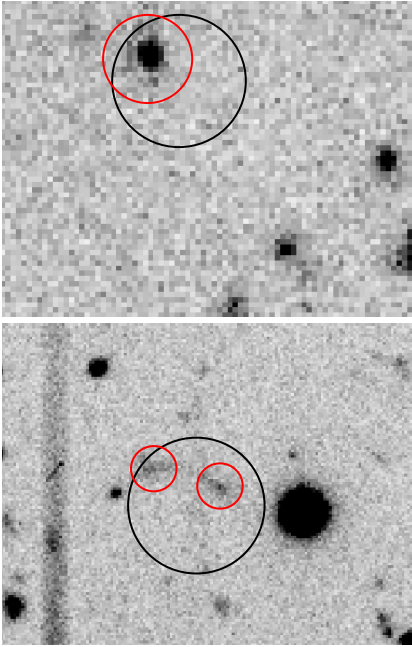


Fig. 1. R-band optical image with superimposed the XMM-Newton error circle. *Upper panel:* a secure identification of an X-ray source on-axis: the XMM-Newton error circle radius (large circle) is $3''$, while the ERO counterpart is indicated by the small circle ($2''$). *Lower panel:* the ambiguous identification of an X-ray source off-axis: the XMM-Newton error circle has a $6''$ radius, while the positions of two possible counterparts (both of them EROs) are indicated with the smaller $2''$ circles.

clustering analyses of the ERO population.

We have started an extensive program of multiwavelength observations of the largest sample of EROs available to date (~ 450 sources), selected in a contiguous area over a ~ 700 arcmin² field (the “Daddi field”, Daddi et al. 2000) and complete to a magnitude limit of $K=19.2$. Deep optical ($R \sim 26.2$ at the 3σ level) photometry is available for the present field (see Daddi et al. 2000 for details in optical and near-infrared data reduction) and VIMOS spectroscopy is planned at VLT. Here we present preliminary results from the first 25 ks XMM-Newton observation of this field (Sec. 2) and compare our results with other recent findings from medium and deep hard X-ray surveys (Sec. 3). Finally, we try to draw some conclusions on the nature of hard X-ray selected EROs (Sec. 4).

2. Data reduction and results

The Daddi field was observed on August 3, 2001 for a nominal exposure time of ~ 50 ks.

The XMM-Newton data were processed using version 5.2 of the Science Analysis System (SAS). The event files were cleaned up from hot pixels and soft proton flares, removing all the time intervals with a count rate higher than 0.15

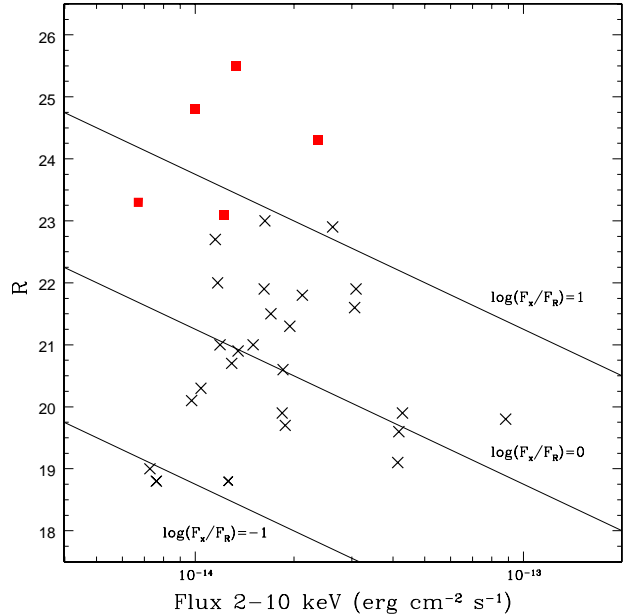


Fig. 2. R-band magnitude vs. hard X-ray flux for the 31 sources with K -band counterparts detected in the XMM-Newton observation. Filled squares are EROs. The solid lines represent loci of equal X-ray-to-optical flux ratio (0.1, 1, 10).

c/s in the 10–12.4 keV energy range for the two MOS and higher than 0.35 c/s in the 10–13 keV band for the pn unit. The resulting exposure times are ~ 26 ks in the MOS1 and MOS2 detectors and ~ 30 ks in the pn detector. The *EBOXDETECT* task, the standard *SAS* sliding box cell detect algorithm, was run on the 2–10 keV cleaned event. Thirty-six sources were detected above the 3.5σ level, corresponding to a flux limit of $\sim 7 \times 10^{-15}$ erg cm⁻² s⁻¹ assuming a power-law spectrum with $\Gamma=1.8$ and Galactic absorption ($N_H = 5 \times 10^{20}$ cm⁻²).

The X-ray centroids have been corrected for systematic errors with respect to the optical positions of three bright quasars already known in the field (from NED database) and then were cross correlated with the K -band catalog. We searched for near-infrared counterparts within a radius of $3''$ from the X-ray position in the inner region of the XMM-Newton field-of-view (10 arcmin), while for the objects detected at larger off-axis angles we adopted a searching radius of $6''$ to take into account the broadening of the XMM-Newton PSF at increasing distance from the aim point. All but five of the hard X-ray selected sources have at least one counterpart in the K -band image. The number of expected spurious sources, computed from K -band galaxy surface density (Daddi et al. 2000) is about 3. We found a unique candidate for 24 sources (4 of them with $R-K > 5$), while for the remaining 7 objects (most of them at large off-axis angles) we detected two possible counterparts. In one of these cases the 2 optical

counterparts have similar R band magnitudes and EROs colors (Fig. 1); for the purposes of the present paper we consider the nearest ERO as the counterpart of the X-ray source.

Five of the 31 hard X-ray selected sources with near-infrared counterparts are thus tentatively associated with EROs. A more detailed discussion on the XMM-Newton data analysis, the associations of X-ray sources with optical counterparts and the analysis of X-ray colors is reported in Brusa et al. (2002).

The hard X-ray and optical fluxes of the X-ray sources with a K-band counterpart are reported in Fig. 2. All the EROs detected in the XMM-Newton observation show relatively high X-ray-to-optical flux ratios ($f_X/f_O \sim 10$) compared to those of the other X-ray detected sources.

The XMM-Newton field of view covers an area including ~ 350 EROs: the fraction of X-ray active EROs in this optically selected sample is therefore $\sim 1.5\%$ ($5/350$); on the other hand, the fraction of hard X-ray sources with EROs colors is much higher, $\sim 15\%$ ($5/36$), and is in agreement with other XMM-Newton findings (Lehmann et al. 2001).

3. Comparison with literature samples

In order to investigate the nature of hard X-ray selected EROs and the link between faint hard X-ray sources and the ERO population, we have collected all the multiwavelength data available in literature for EROs serendipitously discovered both in XMM-Newton and Chandra medium-deep observations:

- Thirteen EROs detected in the 2–8 keV band in the Chandra Deep Field North observation (Alexander et al. 2002¹, Hornschemeier et al. 2001);
- Five hard X-ray selected EROs serendipitously detected in medium-deep Chandra observations in the fields of SSA13 (Mushotzky et al. 2000), A370 (Barger et al. 2001), and A2390 (Cowie et al. 2001, Crawford et al. 2001);
- Eleven EROs detected in the hard (2–10 keV) band in the XMM-Newton Lockman Hole observation (Mainieri et al. 2002b)

The total sample consists of 34 objects, including the 5 EROs discussed in the present work.

The R-band magnitudes plotted versus the 2–8 keV fluxes are reported in Fig. 3. The X-ray fluxes have been converted into the 2–8 keV energy range, assuming the spectral models quoted in the literature, while the R-band magnitudes have been obtained from published I-band magnitudes adopting $R - I = 1.3$ (Alexander et al. 2002).

The present EROs sample span a wide range of optical

¹ These authors adopted different criteria in the EROs definition: $I - K > 4$, which roughly correspond to $R - K > 5.3$.

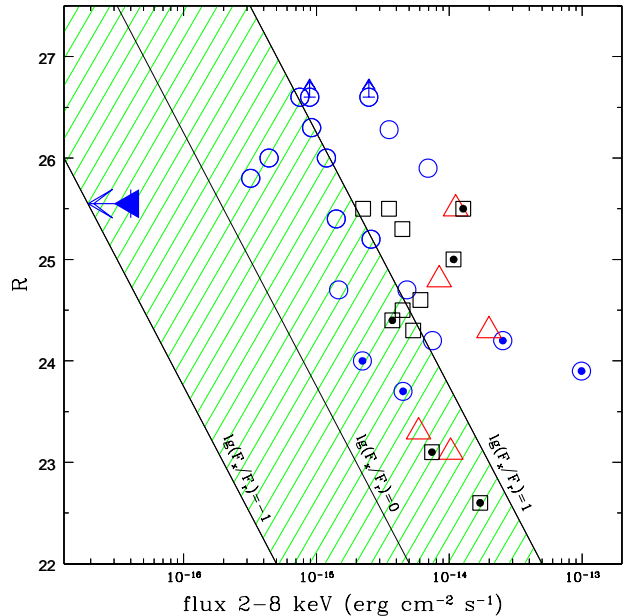


Fig. 3. R-band magnitude vs. hard X-ray flux for a sample of literature EROs, serendipitously detected in hard X-ray surveys. Circles refer to Chandra observations, squares to XMM-Newton Lockman Hole observation, and triangles to the present data. Dot-filled symbols are identified objects (mostly highly obscured, high-luminosity Type II AGN). Open symbols correspond to unidentified objects. For comparison, we report the result of stacking analysis performed on all the EROs in the HDF-N field not individually detected in the Chandra observation (Alexander et al. 2002; upper limit at the faintest X-ray flux).

and X-ray fluxes: all of the objects show a relatively well-defined correlation between the X-ray fluxes and the optical magnitude around $f_X/f_O \simeq 10$. This correlation is shifted by one order of magnitude from the one found by ROSAT for soft X-ray selected quasars (Hasinger et al. 1998) and recently extended by Chandra and XMM-Newton observations also for hard X-ray selected sources (Alexander et al. 2002; Lehmann et al. 2001).

The most plausible explanation of such a high X-ray-to-optical flux ratio in these objects is the presence of high obscuration towards the active nuclear source.

This hypothesis is strongly supported both by X-ray spectral analysis (Gandhi et al. 2001, 2002; Alexander et al. 2002; Cowie et al. 2001; Mainieri et al. 2002a,b) and by the optical identifications available for 9 objects of this sample: all but one of the sources are identified with Type II AGN at $z > 0.7$, either from optical spectroscopy (4 objects) or from deep multi-band photometry (4 objects) (Cowie et al. 2001; Mainieri et al. 2002b; Hornschemeier et al. 2001). The only source not classified as a type II AGN

is the $z=1.020$ emission-line galaxy in the Hornschemeier et al. sample (see their Table 10).

4. Discussion and conclusions

All the findings discussed above support the idea that a significant fraction of the optical counterparts of hard X-ray selected sources are EROs. Indeed, the fraction of EROs among the hard X-ray sources in the Daddi field is $\sim 15\%$; this value rises up to $\sim 25\%$ in the deeper ($F_{2-10\text{keV}} \sim 2 \times 10^{-15} \text{ erg cm}^{-2} \text{ s}^{-1}$) XMM-Newton survey of the Lockman Hole, and has to be considered as a lower limit, as several X-ray sources are not covered by deep near-infrared observations. Interestingly enough, if we consider only the sources with $f_X/f_O > 10$, the fraction of EROs is even higher (more than 50% in the Lockman Hole observation, Mainieri et al. 2002a). The so far identified EROs have high X-ray luminosity ($L_X > 10^{44} \text{ erg s}^{-1}$) and they actually are heavily obscured AGN, as inferred from X-ray spectral analysis (Cowie et al. 2001; Gandhi et al. 2002; Mainieri et al. 2002a). Therefore, hard X-ray selected EROs (or at least a fraction of them) have properties similar to those of Quasars 2, the high-luminosity, high redshift type II AGNs predicted in X-Ray Background (XRB) synthesis models (e.g. Comastri et al. 1995).

Deep optical and near-infrared follow-up of complete samples of hard X-ray selected sources with extreme f_X/f_O will definitively assess the fraction of reddened sources among the XRB constituents.

On the other hand, the fraction of hard X-ray sources within optically selected ERO samples is much lower. At the optical and X-ray flux limits of our survey, the fraction is $\sim 1.5\%$ and rises up to $\sim 15\%$ in the deep 1 Ms CDF-N survey (Alexander et al. 2002). However, it is unlikely that this fraction is much higher than this value. Indeed, the stacking analysis of EROs in the HDF-N actually confirms the lack of hard X-ray emission at fluxes $< 4 \times 10^{-17} \text{ erg cm}^{-2} \text{ s}^{-1}$, with an average f_X/f_O value which is at least two order of magnitudes lower than the average ratio of the individually X-ray detected EROs (Fig. 3). The upper limit on the average f_X/f_O value is consistent with that of passive evolving ellipticals or dusty starbursts suggesting the lack of strong AGN activity in the majority of optically selected EROs.

Deeper X-ray observations of large samples of K -selected EROs would be crucial to compute the fraction of X-ray active EROs on the widest area possible (to avoid cosmic variance). A detailed study of the clustering properties of these objects would shed new light on the link between nuclear activity and galaxy evolution.

Acknowledgements. This research has been partially supported by ASI contracts I/R/103/00, I/R/107/00 and I/R/27/00, and by the MURST grant Cofin-00-02-36. CV also thanks the NASA LTSA grant NAG5-8107 for financial support. We

gratefully thank D. Alexander, G. Zamorani and F. Fiore for useful discussions and V. Mainieri for providing data prior to publication.

References

- Alexander D.M., Vignali C., Bauer F.E., Brandt W.N., Hornschemeier A.E., Garmire G.P., & Schneider D.P., 2002, AJ 123, 1149
- Almaini O., et al., 2002, MNRAS submitted, astro-ph/0108400
- Barger A.J., Cowie L.L., Bautz M.W., Brandt W.N., Garmire G.P., Hornschemeier A.E., Ivison R.J., & Owen F.N., 2001, AJ 122, 2167
- Brusa M., Comastri A., Daddi E., et al., 2002, in preparation
- Cimatti A., Andreani P., Rottgering H., & Tilanus R., 1998, Nature 392, 895
- Cimatti A., et al. 2002, A&A 381, L68
- Comastri A., Setti G., Zamorani G., & Hasinger G., 1995, A&A 296, 1
- Cowie L.L., et al., 2001, ApJ 551, L9
- Crawford C.S., Fabian A.C., Gandhi P., Wilman R.J., & Johnstone R.M., 2001, MNRAS 324, 427
- Daddi E., Cimatti A., Pozzetti L., Hoekstra H., Röttgering H.J.A., Renzini A., Zamorani G. & Mannucci F., 2000, A&A 361, 535
- Daddi E., Cimatti A., & Renzini A., 2000, A&A 362, L45
- Daddi E., et al. 2002, A&A 384, L1
- Elston R., Rieke G.H., & Rieke M.J., 1988, ApJ 331, L77
- Gandhi P., Crawford C.S., Fabian A.C., Wilman R.J., Johnstone R.M., Barger A.J., & Cowie L.L., 2001, Proc. XXI Moriond Astrophysics Meeting, "Galaxy Clusters and the High Redshift Universe Observed in X-rays", eds D. Neumann, F. Durret & J. Tran Thanh Van, astro-ph/0106139,
- Gandhi P., Fabian A.C., & Crawford C.S., 2002, Proc. Symposium 'New Visions of the X-ray Universe in the XMM-Newton and Chandra Era', ESA SP-488, August 2002 ed. F. Jansen, astro-ph/0201543
- Granato G.L., Silva L., Monaco P., Panuzzo P., Salucci P., De Zotti G., Danese L., 2001, MNRAS 324, 757
- Hasinger G., et al., 1998, A&A 329, 482
- Hornschemeier A.E., et al. 2001, ApJ 554, 742
- Lehmann I., Hasinger G., Murray S.S. & SchmidtLehmann M., 2001, Proceedings for "X-rays at Sharp Focus Chandra Science Symposium", astro-ph/0109172
- Mainieri V., Bergeron J., Rosati P., Hasinger G., & Lehmann I., 2002a, astro-ph/0202211, Proc. Symposium 'New Visions of the X-ray Universe in the XMM-Newton and Chandra Era', ESA SP-488, August 2002 eds. F. Jansen
- Mainieri V., et al., 2002b, in preparation
- Mushotzky R.F., Cowie L.L., Barger A.J., & Arnaud K.A., 2000, Nature 404, 459
- Pierre M., et al., 2001, A&A 372, L45
- Smail I., Ivison R.J., Kneib J.P., Cowie L.L., Blain A.W., Barger A.J., Owen F.N., & Morrison G., 1999, MNRAS 308, 1061